Chapter 9
The Properties of Neutrinos

This chapter deals with the physics of neutrinos, which are neutral particles, partners of the charged leptons in SU(2) *multiplets, subject to the weak interaction only—besides their negligible gravitational interaction. Due to their low interaction probability, they are very difficult to detect and as a consequence the neutrino sector is the least known in the standard model of particle physics. In the late 1990s it has been discovered that neutrinos of different flavors (electron, muon, or tau) "oscillate": neutrinos created with well-defined leptonic flavor may be detected in another flavor eigenstate. This phenomenon implies that neutrinos have a non-zero—although tiny even for the standards of particle physics—mass.*

Neutrinos have been important for the developments of particle physics since they were conjectured in the 1930s and are still at present at the center of many theoretical and experimental efforts. Their detection is difficult, since they are only subject to weak interactions (besides the even weaker gravitational interaction).

The existence of neutrinos was predicted by Wolfgang Pauli in 1930 in order to assure the energy–momentum conservation in the β decay as it was recalled in Sect. 2.3. Then in 1933 Enrico Fermi established the basis of the theory of weak interactions in an analogy with QED but later on it was discovered that parity is not conserved in weak interactions: neutrinos should be (with probability close to one) left-handed, and antineutrinos should be right-handed (see Chap. 6). The theory needed a serious update, which was performed by the electroweak unification (Chap. 7).

Neutrinos were experimentally discovered only in the second-half of the twentieth century: first the electron antineutrino in 1956 by Reines[1] and Cowan (Sect. 2.3); then

[1] Frederick Reines (1918–1998) was a physicist from the USA, professor at the University of California at Irvine and formerly employed in the Manhattan project. He won the Nobel Prize in Physics 1995 "for pioneering experimental contributions to lepton physics"; his compatriot and coworker Clyde Cowan Jr. (1919–1974) had already passed away at the time of the recognition.

A. De Angelis and M. Pimenta, *Introduction to Particle and Astroparticle Physics*, Undergraduate Lecture Notes in Physics,
https://doi.org/10.1007/978-3-319-78181-5_9

in 1962 the muon neutrino by Lederman, Schwartz, and Steinberger[2]; and finally, the tau neutrino in 2000 by the DONUT experiment at Fermilab (Sect. 5.6.2). Meanwhile it was established in 1991 in the LEP experiments at CERN that indeed there are only three kinds of light neutrinos (see Sect. 7.5.1).

Neutrinos are only detected through their interactions, and different neutrino flavors are defined by the flavors of the charged lepton they produce in weak interactions. The electron neutrino ν_e, for example, is the neutrino produced together with a positron, and its interaction will produce an electron - and similarly for the muon and the tau neutrinos.

For many years it was thought that neutrinos were massless, and for the standard model of particle physics three generations of massless left-handed neutrinos were enough—a nonzero mass was not forbidden, but it implied new mass terms in the Lagrangian discussed in Chap. 7. There was anyway a "cloud": the so-called solar neutrino problem—in short, the number of solar electron neutrinos arriving to the Earth was measured to be much smaller (roughly between one-third and 60%, depending on the experiment's threshold) of what it should have been according to the estimates based on the solar power. This problem was solved when it was demonstrated that neutrinos can change flavor dynamically: neutrino species "mix," and quantum mechanics implies that, since they mix, they cannot be massless.

9.1 Sources and Detectors; Evidence of the Transmutation of the Neutrino Flavor

Neutrinos are generated in several processes, and their energy spans a wide range (Fig. 9.1). Correspondingly, there are different kinds of detectors to comply with the different fluxes and cross sections expected.

Let us start by analyzing some neutrino sources. Solar, atmospheric, reactor, and accelerator neutrinos have been complementary in determining the neutrino oscillation parameters, and thus, constraining the masses and the mixing matrix. Other sources of neutrinos, more relevant for astrophysics, will be discussed in Chap. 10.

9.1.1 Solar Neutrinos, and the Solar Neutrino Problem

In the so-called Standard Solar Model (SSM), the Sun produces energy via thermonuclear reactions in its core, a region $<10\%$ of the solar radius containing roughly 1/3 of the total mass. Most of the energy is released via MeV photons, which originate

[2]The Nobel Prize in Physics 1988 was awarded jointly to Leon Lederman (New York 1922), Melvin Schwartz (New York 1931—Ketchum, Idaho, 2006), and Jack Steinberger (Bad Kissingen 1921) "for the neutrino beam method and the demonstration of the doublet structure of the leptons through the discovery of the muon neutrino."

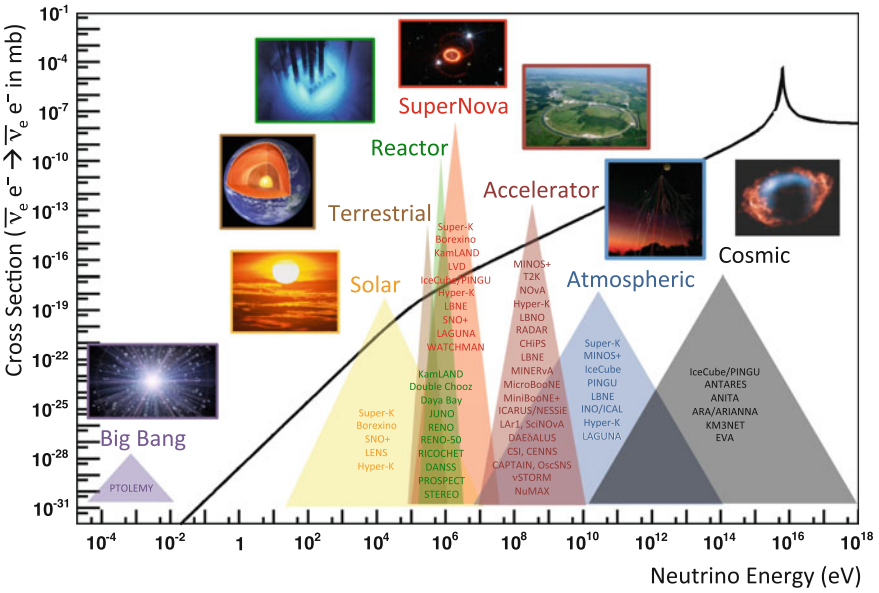

Fig. 9.1 Neutrino interaction cross section as a function of energy, showing typical energy regimes accessible by different neutrino sources and experiments. The curve shows the scattering cross section for an electron antineutrino on an electron. From A. de Gouvêa et al., arXiv:1310.4340v1

the electromagnetic solar radiation through propagation and interaction processes that take a long time (∼2 million years). The light emitted comes mostly from the thermal emission of the external region, the photosphere, which has a temperature of about 6000 K, and is heated by the moderation of these photons.

The fusion reactions in the Sun release about 26.7 MeV and produce also a large flux of electron neutrinos that can be detected at Earth (the expected flux at Earth predicted by John Bahcall and collaborators in the SSM is $\sim 6 \times 10^{10}$ cm^{-2}s^{-1}). This flux is produced mainly by the nuclear reactions initiated by proton–proton (pp) fusions as sketched in Fig. 9.2. The contribution of the alternative CNO chain[3] is small.

The dominant pp reaction (>90% of the total flux) produces ν_e which have a low energy endpoint (<0.42 MeV) as it is shown in Fig. 9.3. The ^{7}B line at 0.86 MeV is the second most relevant ν_e source (7–8%) while the "pep" reaction producing ν_e with energy of 1.44 MeV contributes with just a 0.2%.

^{8}B neutrinos are produced in the "$ppIII$" chain with energies <15 MeV and although their flux could appear marginal (∼0.1%) they have a major role in the

[3]The CNO cycle (for carbon–nitrogen–oxygen) is a set of alternative chains of conversion of hydrogen to helium. In the CNO cycle, four protons fuse, giving origin to one alpha particle, two positrons and two electron neutrinos; the cycle uses C, N, and O as catalysts. While the threshold of the pp-chain is around temperatures of 4 MK, the threshold of a self-sustained CNO chain is at approximately 15 MK. The CNO chain becomes dominant at 17 MK.

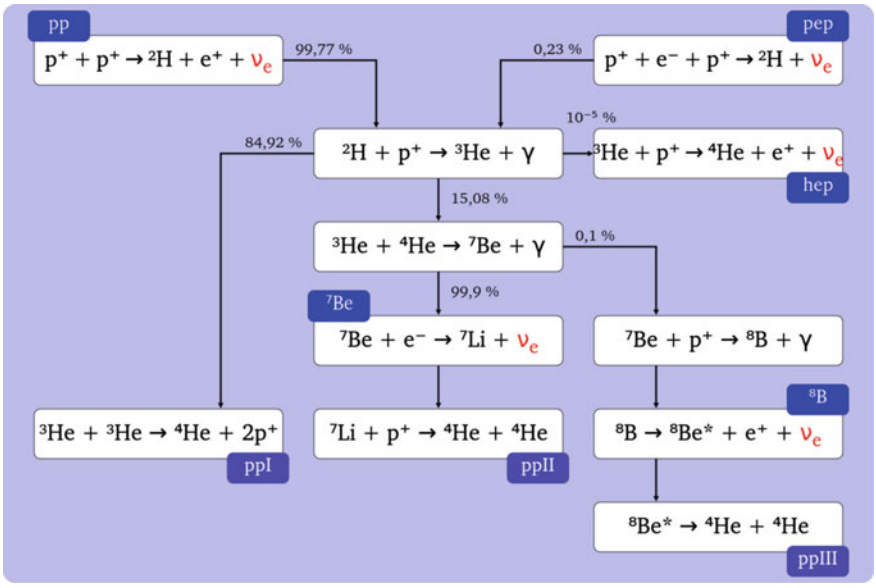

Fig. 9.2 Main nuclear fusion reactions that contribute to the solar neutrino flux. By Dorottya Szam [CC BY 2.5 http://creativecommons.org/licenses/by/2.5], via Wikimedia commons

solar neutrino detection experiments. In fact, they were the dominant contribution in the historical Chlorine experiment and can be detected by Cherenkov experiments like Super-Kamiokande and SNO (Fig. 9.3).

The first solar neutrino experiment was done in the late 1960s by Ray Davis in the Homestake mine in South Dakota, USA, counting the number of ^{37}Ar atoms produced in 615 ton of C_2Cl_4 by the reaction involving chlorine:

$$\nu_e \, {}^{37}_{17}\mathrm{Cl} \rightarrow {}^{37}_{18}\mathrm{Ar} \, e^- \tag{9.1}$$

(Nobel prize for Davis, as we discussed in Chap. 4). The observed rate was just around one-third of the expected number of interactions based on the energetics of the Sun. This unexpected result originated the so-called solar neutrino problem that for three decades led to a systematic and careful work of a large community of physicists, chemists, and engineers which finally confirmed both the predictions of the SSM and the experimental results of Davis: the explanation was in a fundamental property of neutrinos. Indeed subsequent solar neutrino experiments based on different detection techniques also found a significant deficit in the observed ν_e fluxes; in particular, the GALLEX (at the INFN laboratories under Gran Sasso in Italy) and the SAGE (at Baksan in Russia) experiments used also a radiochemical technique with a lower threshold, choosing Gallium as the detection medium, enabling thus the detection of *pp* neutrinos.

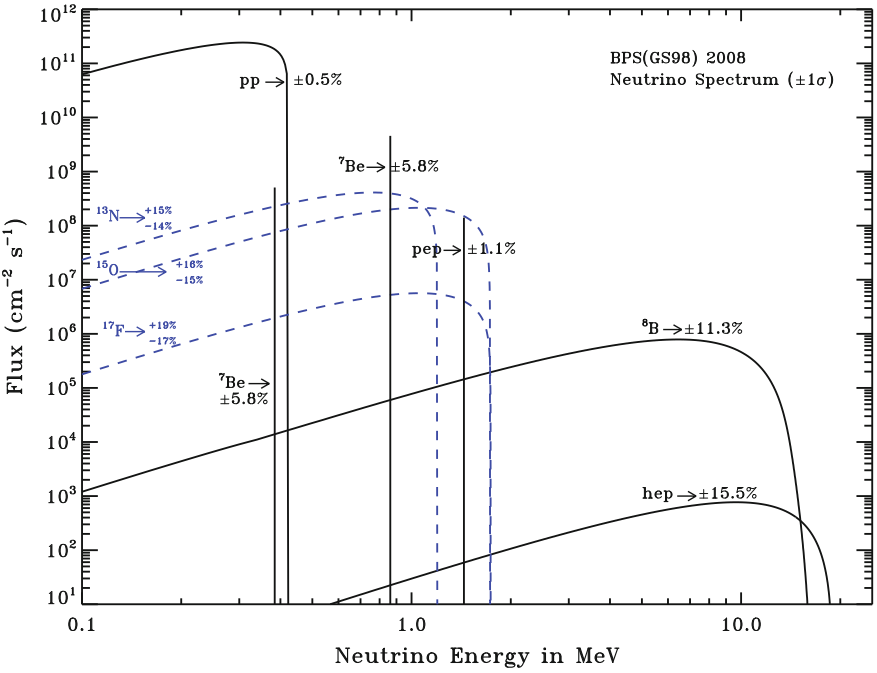

Fig. 9.3 Solar neutrino energy spectrum predicted by the SSM. For continuum sources, fluxes are expressed in units of $cm^{-2}s^{-1}$ MeV^{-1} at the Earth's surface. For line sources, the units are number of neutrinos $cm^{-2}s^{-1}$. The total theoretical errors are quoted for each source. From arxiv.org/abs/0811.2424

The Kamiokande and the Super-Kamiokande (described in Chap. 4; also called Super-K, or SK) experiments at Kamioka in Japan used water as target material (50 000 tons in the case of Super-K) which allowed the detection, by Cherenkov radiation, of electrons produced in the interaction of MeV neutrinos on atomic electrons. The energy and the direction of the scattered electron could be measured determining, respectively, the number of photons and the orientation of the Cherenkov ring. In this way, as the electron keeps basically the direction of the incoming neutrino, it could be proved that indeed the neutrinos were coming from the Sun as it is shown by the beautiful "neutrino picture" of the Sun (Fig. 9.4) that was obtained.

Also in this experiment the total observed flux, when interpreted as only ν_e interactions, is significantly lower than expected by the SSM.

Was the SSM wrong, or some electron neutrinos were disappearing on their way to the Earth? The final answer was given by the Sudbury Neutrino Observatory (SNO) in Canada. SNO used 1000 tons of heavy water (D_2O) as target material. Both charged- and neutral-current neutrino interactions with deuterium nuclei were then observable:

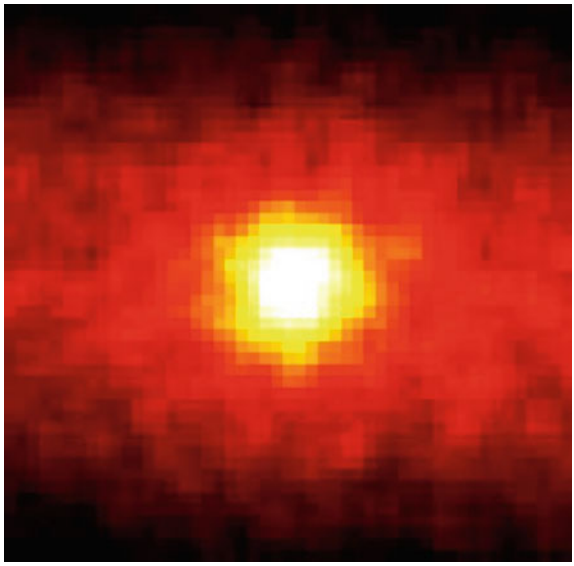

Fig. 9.4 Image of the Sun obtained in a 500 days run of Super-Kamiokande. R. Svoboda and K. Gordan (Louisiana State University, USA)

- $\nu_e\, d \rightarrow e^-\, p\, p$ (charged current, CC);
- $\nu_x\, d \rightarrow \nu_x\, n\, p$ (neutral current, NC).

While in the first reaction only the ν_e can interact (the neutrino energy is below the kinematic threshold for tau production), the neutrinos of all flavors can contribute to the second one. The resulting e^- is detected by measuring the corresponding water Cherenkov ring. The neutron in the final state may be captured either with low efficiency in the deuterium nuclei or with higher efficiency in ^{35}Cl nuclei from 2 tons of salt (NaCl) that were added in the second phase of the experiment. In any case in those radiative captures γ photons are produced and these may produce, via Compton scattering, relativistic electrons which again originate Cherenkov radiation. In the third and final phase, an array of ^{3}He-filled proportional counters was deployed to provide an independent counting of the NC reaction. In addition to the two processes described above, the elastic scattering

$$\nu_x e^- \rightarrow \nu_x e^-$$

is also possible for all neutrino types—although with different cross sections, being the neutrino electron process favored with respect to the other neutrino types.

While ν_e, ν_μ, ν_τ can contribute to the NC, only ν_e contribute to the CC. Thus one has in SNO a clear way to separate the measurement of the ν_e flux from the measurement of the different active neutrino species (in a three-flavor model, $\nu_e + \nu_\mu + \nu_\tau$). SNO could determine that

$$\frac{\Phi(\nu_e)}{\Phi(\nu_x)} = 0.340 \pm 0.038\ (\text{stat.} + \text{syst.})$$

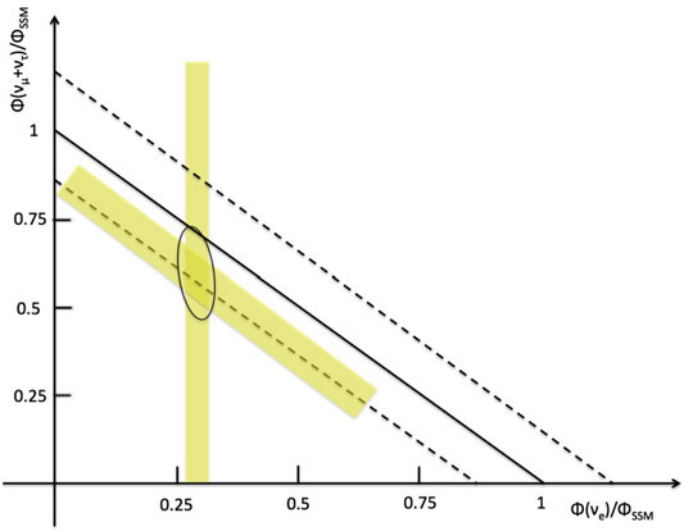

Fig. 9.5 Flux of muon plus tau neutrinos versus the flux of electron neutrinos as derived from the SNO data. The vertical band comes from the SNO charged-current analysis; the diagonal band from the SNO neutral-current analysis; the ellipse shows the 68% confidence region from the best fit to the data. The predicted Standard Solar Model total neutrino flux is the solid line lying between the dotted lines

and thus indicated that electron neutrinos might transform themselves into different neutrino flavors during their travel from the Sun to the Earth. The result is compatible with a value of 1/3.

The results obtained by SNO are summarized in Fig. 9.5. The total measured neutrino flux is clearly compatible with the total flux expected from the SSM and the fraction of detected ν_e is consistent with being only one-third of the total number of the neutrinos.

The solar neutrino problem could be solved without modifying the SSM, and the solution was that solar neutrinos change their flavor during their way to the Earth; the mixing appears to be maximal, in the sense that electron neutrinos are only one-third of the total.

Let us examine now the characteristics of the oscillation of neutrinos in the simplified hypothesis that there are only two flavors and two eigenstates.

9.1.2 Neutrino Oscillation in a Two-Flavor System

The transmutation of neutrinos from one species to another implies in a quantum mechanical world an oscillation phenomenon, similar to what we have observed in the

$K^0 - \bar{K}^0$ system. We examine now a simplified model of the neutrino oscillations, to see its implications.

In a world with two flavors (let us suppose for the moment they are ν_e, ν_μ) and two mass (ν_1, ν_2) eigenstates, the flavor eigenstates can be written as a function of a single real mixing angle θ as:

$$\nu_e = \nu_1 \cos\theta + \nu_2 \sin\theta \tag{9.2}$$

$$\nu_\mu = -\nu_1 \sin\theta + \nu_2 \cos\theta \tag{9.3}$$

or, using matrices,

$$\begin{pmatrix} \nu_e \\ \nu_\mu \end{pmatrix} = \begin{pmatrix} \cos\theta & \sin\theta \\ -\sin\theta & \cos\theta \end{pmatrix} \begin{pmatrix} \nu_1 \\ \nu_2 \end{pmatrix} . \tag{9.4}$$

Then, for instance, if a ν_e is produced at time $t = 0$ and position $\mathbf{x} = 0$, the space–time evolution of this quantum state ψ will be determined by the evolution of the corresponding mass eigenstates:

$$\psi = \nu_1 \cos\theta e^{-i(E_1 t - \mathbf{p_1}.\mathbf{x})} + \nu_2 \sin\theta e^{-i(E_2 t - \mathbf{p_2}\cdot\mathbf{x})} \tag{9.5}$$

or, expressing this quantum state again in terms of the weak eigenstates:

$$\begin{aligned} \psi = &\left(\cos^2\theta e^{-i(E_1 t - \mathbf{p_1}.\mathbf{x})} + \sin^2\theta e^{-i(E_2 t - \mathbf{p_2}.\mathbf{x})}\right)\nu_e - \\ &\left(\cos\theta \sin\theta \left(e^{-i(E_1 t - \mathbf{p_1}.\mathbf{x})} - e^{-i(E_2 t - \mathbf{p_2}.\mathbf{x})}\right)\right)\nu_\mu . \end{aligned}$$

Note that at ($t = 0$, $\mathbf{x} = 0$), $\psi = \nu_e$ but, at later times, there will be usually a mixture between the two-flavor states ν_e, ν_μ.

It can be seen from the equations above that the probability to find a state ν_μ at a distance L from the production point is given by:

$$P\left(\nu_e \to \nu_\mu\right) = \sin^2(2\theta) \sin^2\left(\frac{\Delta m^2 L}{4E_\nu}\right) \tag{9.6}$$

where

$$\Delta m^2 = \left(m_2^2 - m_1^2\right) . \tag{9.7}$$

In order for the mixing to have an effect, the two masses must be different; i.e., at least one should be different from zero. The $\sin^2(2\theta)$ factor plays the role of the amplitude of the oscillation while the phase is given by $\Delta m^2 L/4E_\nu$. A phase too small or too large makes the measurement of the oscillation parameters quite difficult. Typically, an experiment is sensitive to:

$$\left|\Delta m^2\right| \sim \frac{E_\nu}{L} . \tag{9.8}$$

It is also usual to define an oscillation length L_ν as:

$$L_\nu = \frac{2\pi E_\nu}{\Delta m^2} \tag{9.9}$$

and then

$$P\left(\nu_e \to \nu_\mu\right) = \sin^2(2\theta)\sin^2\left(\frac{\pi}{2}\frac{L}{L_\nu}\right). \tag{9.10}$$

We stress the fact that, whenever $L \sim n\,L_\nu$ (with $n = 1, 3, \ldots$), the probability of oscillation is maximal.

The oscillation formula is often written using practical units:

$$P\left(\nu_e \to \nu_\mu\right) = \sin^2(2\theta)\sin^2\left(1.27\,\frac{\Delta m^2\,(\mathrm{eV}^2)\,L\,(\mathrm{km})}{E_\nu\,(\mathrm{GeV})}\right) \tag{9.11}$$

and the probability to find a state ν_e at the same distance L is by construction:

$$P\left(\nu_e \to \nu_e\right) = 1 - P\left(\nu_e \to \nu_\mu\right). \tag{9.12}$$

The oscillation probabilities, in this two-flavor world, are just a function of two parameters: the mixing angle θ and the difference of the squares of the two masses $\Delta m^2 = \left(m_1^2 - m_2^2\right)$.

Experiments that measure the possible depletion of the initial neutrino beam are called *disappearance* experiments. Experiments that search for neutrinos with a flavor different from the flavor of the initial neutrino beam are called *appearance* experiments. An appearance experiment is basically sensitive to a given oscillation channel $\nu_i \to \nu_j$ with $i \neq j$ while a disappearance experiment is sensitive to transitions to all possible different neutrino species, or to pure disappearance.

The determination of the parameters of neutrino oscillations has been one of the priorities of the research during the recent years. If neutrinos oscillate, their masses, although small, cannot be zero. The direct measurement of such masses and of the mixing strengths has gained a renewed interest.

The theoretical origin of neutrino masses is not yet established: either it is the result of the Higgs mechanism as it is the case for all the other fermions (Dirac neutrino) or, as suggested by Majorana, the neutrino is its own antiparticle (Majorana neutrino). If the latter is the case, double beta decays—nuclear decays in which two neutrons become protons—could be neutrinoless (the simplest way of viewing this fact is to think that the two neutrinos annihilate each other, or that the second neutron absorbs the neutrino emitted by the first one during its transition, and then undergoes the process $\nu n \to p$).

In addition, neutrinos travel a long way within the Sun, and most of the neutrino oscillation is likely to happen in matter.

The neutrino oscillations can be enhanced (or suppressed) whenever neutrinos travel through matter. In fact, while all neutrino flavors interact equally with matter

through neutral currents, charged-current interactions with matter are flavor dependent (at solar neutrino energies, basically only electron neutrinos can interact). This is called the MSW effect, as it comes from works by Lincoln Wolfenstein, Stanislav Mikheyev, and Alexei Smirnov. Thus, the time evolution in matter of the electron neutrino and of the other neutrinos can be different.

In the case of a constant density medium, this effect is translated, in a two-flavor approximation, into a modified oscillation probability $\nu_e \to \nu_x$:

$$P\left(\nu_e \to \nu_x\right) = \sin^2\left(2\theta_m\right) \sin^2\left(\frac{\pi}{2}\frac{L}{L_\nu}F\right) \tag{9.13}$$

where

$$\sin\left(2\theta_m\right) = \sin\left(2\theta\right)/F, \tag{9.14}$$

$$F = \sqrt{\left(\cos\left(2\theta\right) - \frac{L_\nu}{L_e}\right)^2 + \sin^2\left(2\theta\right)} \tag{9.15}$$

and

$$L_e = \pm 2\pi / \left(2\sqrt{2} G_F N_e\right). \tag{9.16}$$

L_e, the electron neutrino interaction length, is positive for neutrinos, negative for antineutrinos. G_F is the Fermi constant, and N_e is the electron density in the medium. L_ν, the neutrino oscillation length in vacuum, is, as defined before, a function of the neutrino energy and of the difference of the square of the masses:

$$L_\nu = \frac{2\pi E_\nu}{\Delta m^2}. \tag{9.17}$$

Note that the sign of L_ν is determined by the sign of Δm^2. In fact as it will be discussed in Sect. 9.2 there are two possibilities in the hierarchy of the neutrino masses and thus the sign of Δm^2 can be positive or negative.

The values of the mass eigenstates are also changed. The new eigenstates are given by:

$$M_{2,1}^2 = \frac{1}{2}\left[m_1^2 + m_2^2 + \Delta m^2\left(\frac{L_\nu}{L_e} \pm F\right)\right] \tag{9.18}$$

where the $+$ sign is for M_2 and the $-$ is for M_1. Whenever $L_\nu = L_e \cos\left(2\theta\right)$ the amplitude of the oscillation is maximal ($\sin^2\left(2\theta_m\right) = 1$). Thus, for a given set of (E, N_e) values, resonant oscillations are possible and the oscillation probability may be strongly enhanced independently of the value of θ in vacuum.

In the center of the Sun $N_e \sim 3 \times 10^{31}\,\mathrm{m}^{-3}$ and then the value of L_e is $\sim 3 \times 10^5$ m which is a small number when compared with the Sun radius (10^8–10^9 m). In this way, the suppression of the electron neutrinos is a function of the neutrino energy for given values of Δm^2 and θ.

How to determine the oscillation parameters? More information comes from different neutrino sources.

9.1.3 *Long-Baseline Reactor Experiments*

Nuclear reactors are abundant $\overline{\nu}_e$ sources via the β decays of several of the isotopes produced in the fission reactions. The $\overline{\nu}_e$ have an energy of a few MeV and can be detected by the inverse β decay reaction ($\overline{\nu}_e\ p \rightarrow e^+ n$). The results from reactors can be combined with the results obtained in the solar experiments supposing that ν_e and $\overline{\nu}_e$ have the same behavior. In reactor experiments the energies and the distances are much better determined than in solar experiments.

The KamLAND experiment (again in Kamioka in Japan), a 1000-ton liquid scintillator detector, is placed at distances of the order of 100 km from several nuclear reactors (the weighted average distance being of 180 km) and thus, as discussed in the previous section, is sensitive to small Δm^2 oscillations.

Electron antineutrinos are detected through the reaction $\bar{\nu}_e p \rightarrow e^+ n$, which has a 1.8 MeV energy threshold. The prompt scintillation light from the positron allows to estimate the energy of the incident antineutrino. The neutron recoil energy is only a few tens of keV; the neutron is captured on hydrogen and a characteristic 2.2 MeV gamma ray is emitted after some 200 μs. This delayed coincidence between the positron and the gamma-ray signals provides a very powerful signature for distinguishing antineutrinos from backgrounds produced by other sources.

KamLAND detects a clear pattern of oscillation as shown in Fig. 9.6.

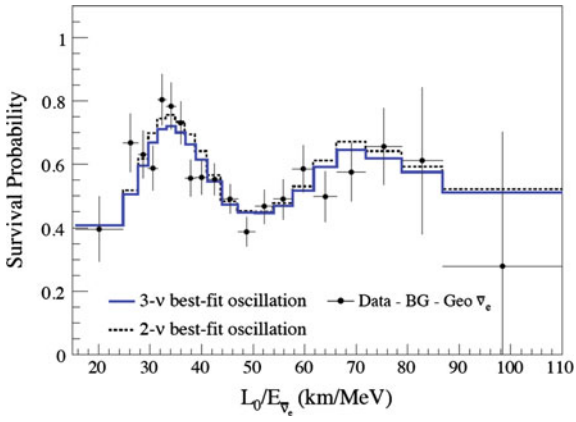

Fig. 9.6 The $\overline{\nu}_e$ survival probability as a function of L/E observed in the KamLAND experiment. Figure from A. Gando et al. (KamLAND Collab.), Phys. Rev. D83 (2011) 052002

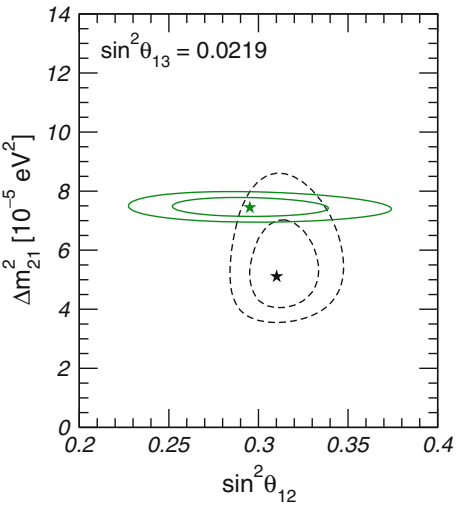

Fig. 9.7 Allowed parameter regions (at 1σ and 2σ) in the $(\sin^2\theta_{12}, \Delta m^2_{21})$ space for the combined analysis of solar neutrino data and for the analysis of KamLAND data. The result for KamLAND is illustrated by the ellipses with horizontal major axis, with the best fit marked by a green star. The two other ellipses and the other star indicate the corresponding values for solar neutrino data. Figure adapted from NuFIT 2017

9.1.4 Estimation of $\nu_e \rightarrow \nu_\mu$ Oscillation Parameters

KamLAND and the solar experiments provide the best determinations of the θ and Δm^2 parameters involved in the ν_e oscillations. The results taking into account all the data available at the end of 2017 are shown in Fig. 9.7, where these parameters are labeled, as it will be discussed later on, as θ_{12} and Δm^2_{21}. There is a perfect agreement in the obtained values of $\sin^2(\theta_{12})$ while the central value of KamLAND for Δm^2_{21} is slightly higher (2σ) than the one from solar experiments. The best-fit values obtained for these parameters in the NuFIT[4] 3.1 (2017) (we shall call them for the moment $\theta_{\rm Sun}$ and $\Delta m^2_{\rm Sun}$) are:

$$\sin^2(2\theta_{\rm Sun}) \sim 0.85\,, \tag{9.19}$$

and

$$\Delta m^2_{\rm Sun} \sim 7.5 \times 10^{-5}{\rm eV}^2\,. \tag{9.20}$$

Note that it is not straightforward to obtain the "solar" parameters listed above from solar neutrino data: large part of the oscillation effect happens within the Sun and needs a different mathematical treatment with respect to the oscillation in vacuo.

[4]The NuFIT group provides and regularly updates at the Web site http://www.nu-fit.org/ a global analysis of neutrino oscillation measurements.

9.1.5 *Atmospheric Neutrinos and the $\nu_\mu \to \nu_\tau$ Oscillation*

Another solid evidence that neutrinos do oscillate came from the measurement at the Earth surface of the relative ratio of the ν_e and ν_μ produced in cosmic-ray showers (Fig. 9.8; see also Chap. 10) by the decays of the $\pi^\pm$ and to a lesser extent of the $K^\pm$. The decay chains:

$$\pi^+ \to \mu^+ \nu_\mu \; ; \; \mu^+ \to e^+ \nu_e \overline{\nu}_\mu \tag{9.21}$$

$$\pi^- \to \mu^- \overline{\nu}_\mu \; ; \; \mu^- \to e^- \overline{\nu}_e \nu_\mu \tag{9.22}$$

imply that the ratio:

$$R = \frac{\nu_\mu + \overline{\nu}_\mu}{\nu_e + \overline{\nu}_e} \tag{9.23}$$

should be around 2. In fact the value of this ratio is slightly different from 2, because not all muons decay in their way to Earth and only around 63% of the $K^\pm$ follow

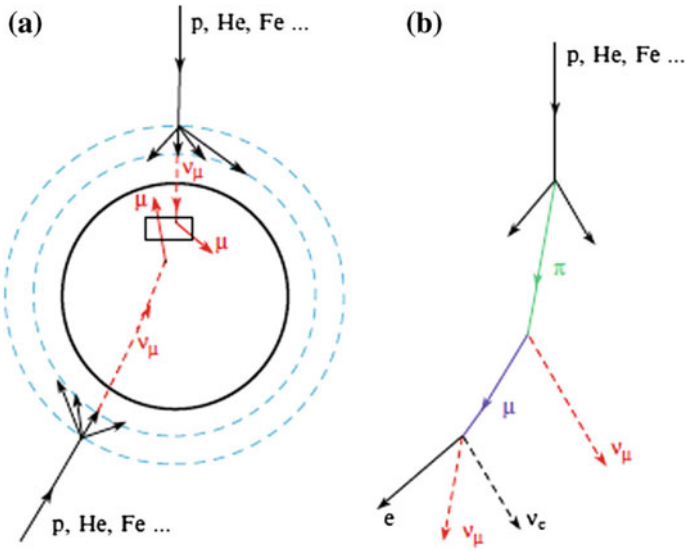

Fig. 9.8 Interaction of cosmic rays in the upper atmosphere generates particle showers comprising neutrinos (right picture), which originate from a 10–20 km thick atmospheric layer. A large volume detector placed underground, like Super-K, is used to detect them; downward-going neutrinos traveled only few tens of kilometers and had no "space" to oscillate, while upward-going neutrinos have traveled about 10 000 km and have likely oscillated. The detector (left picture) can distinguish between electron neutrinos and muon neutrinos: secondary muons are likely to escape the detector (noncontained or partially contained events), while secondary electrons formed by neutrino electrons interacting in the detector are likely to be absorbed (fully contained events). In the case of fully contained events the electron ring is "fuzzier" than the muon ring. From Braibant, Giacomelli and Spurio, "Particles and fundamental interactions," Springer 2014

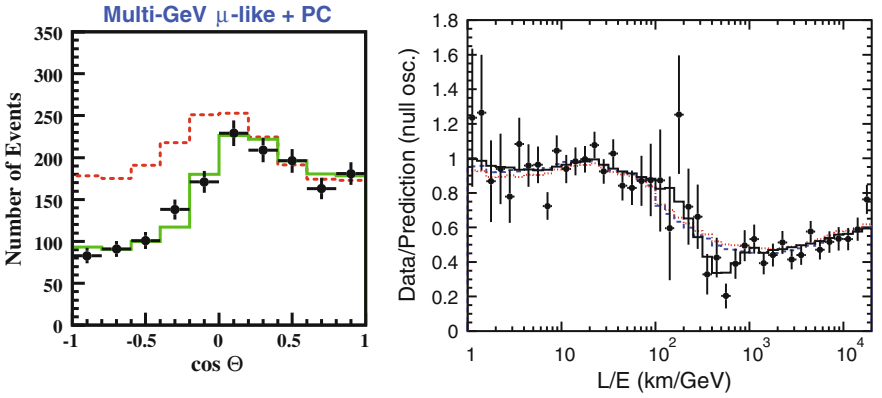

Fig. 9.9 Left: Zenith angle distribution of muon neutrinos in SK. The observed number of upward-going neutrinos was roughly half of the predictions. Right: Survival probability of ν_μ as a function of L/E. Black dots show the observations and the lines shows the prediction based on neutrino oscillation. Data show a dip around $L/E \simeq 500$ km/GeV. The prediction of two-flavor neutrino oscillations agrees well with the position of the dip. From http://www-sk.icrr.u-tokyo.ac.jp/sk/physics/atmnu-e.html and The Super-Kamiokande Collaboration, Y. Ashie et al., "Evidence for an Oscillatory Signature in Atmospheric Neutrino Oscillations," Phys. Rev. Lett. 93 (2004) 101801

similar decay chains; this ratio is, thus, energy-dependent. Monte Carlo calculations allow the computation of these corrections.

The ratio measured by Kamiokande-II, Super-Kamiokande, and by several other experiments, was however quite different from 2. There was, as it is shown in Fig. 9.9, left, a clear deficit of muon neutrinos coming mainly from below the detector. Indeed upward muon neutrinos ($\cos\theta < 0$, see Fig. 9.8) which traveled longer distances showed a higher probability to disappear. As the interaction cross section in the Earth is too small to explain such disappearance (and no deficit was observed for electron neutrinos), this phenomenon is due to muon neutrino oscillation in particular into tau neutrinos.

Since the number of electron neutrinos was found not to deviate from expectations, oscillations were interpreted as indeed mainly involving tau neutrinos (any undetected type of neutrino would anyway explain the observations). In fact the observed modulation pattern as a function of the zenith angle (Fig. 9.9, left) and as a function of L/E (Fig. 9.9, right) is very well reproduced considering the same survival oscillation formula (Eq. 9.11) deduced in just a two-flavor scenario but now between the muon and the tau neutrinos.

The best fit to all available data provides:

$$\Delta m^2_{\text{atm}} \sim 2.5 \times 10^{-3}\text{eV}^2 \tag{9.24}$$

and a large mixing, consistent with unity:

$$\sin^2(2\theta_{\text{atm}}) \sim 1\,. \tag{9.25}$$

We now need to extend the phenomenology of flavor oscillation to three families to see the global picture.

9.1.6 *Phenomenology of Neutrino Oscillations: Extension to Three Families*

Bruno Pontecorvo first suggested in 1957 that the neutrino may oscillate; in the 1960s it was suggested that the neutrino weak and mass eigenstates might have not been the same. Neutrinos would be produced in weak interactions in pure flavor states that would be a superposition of several mass states (preserving unitarity) which would determine their time–space evolution, giving rise to mixed flavor states.

We have shortly discussed in the beginning of this chapter a simplified model in which only two neutrinos and two mass eigenstates appear. Assuming three weak eigenstates (ν_e, ν_μ, ν_τ) and three mass eigenstates (ν_1, ν_2, ν_3), the mixing can be modeled, similarly to what seen for the CKM matrix, using a 3×3 unitary matrix, which we call today the Pontecorvo–Maki–Nakagawa–Sakata (PMNS) matrix

$$\begin{pmatrix} \nu_e \\ \nu_\mu \\ \nu_\tau \end{pmatrix} = \begin{pmatrix} U_{e1} & U_{e2} & U_{e3} \\ U_{\mu 1} & U_{\mu 2} & U_{\mu 3} \\ U_{\tau 1} & U_{\tau 2} & U_{\tau 1} \end{pmatrix} \begin{pmatrix} \nu_1 \\ \nu_2 \\ \nu_3 \end{pmatrix} . \tag{9.26}$$

Taking into account the relations imposed by unitarity and the fact that several phases can be absorbed in the definition of the fields (if the neutrinos are standard fermions) there are only three real parameters usually chosen as the mixing angles θ_{12}, θ_{13}, θ_{23} and a single complex phase written in the form $e^{i\delta}$. If the mixing angle $\theta 13$ and $\sin\delta$ are $\neq 0$, *CP* is violated.

The PMNS matrix can be decomposed as the product of three 3×3 matrices:

$$\begin{pmatrix} U_{e1} & U_{e2} & U_{e3} \\ U_{\mu 1} & U_{\mu 2} & U_{\mu 3} \\ U_{\tau 1} & U_{\tau 2} & U_{\tau 1} \end{pmatrix} = \tag{9.27}$$

$$= \begin{pmatrix} 1 & 0 & 0 \\ 0 & \cos\theta_{23} & \sin\theta_{23} \\ 0 & -\sin\theta_{23} & \cos\theta_{23} \end{pmatrix} \begin{pmatrix} \cos\theta_{13} & 0 & \sin\theta_{13} e^{-i\delta} \\ 0 & 1 & 0 \\ -\sin\theta_{13} e^{i\delta} & 0 & \cos\theta_{13} \end{pmatrix} \begin{pmatrix} \cos\theta_{12} & \sin\theta_{12} & 0 \\ -\sin\theta_{12} & \cos\theta_{12} & 0 \\ 0 & 0 & 1 \end{pmatrix} . \tag{9.28}$$

This format puts in evidence what we observed: in the first approximation, both the oscillation $\nu_e \to \nu_\mu$ and the oscillation $\nu_\mu \to \nu_\tau$ can be described as oscillations between two weak eigenstates and two mass eigenstates. Thus, we can identify the two most important parameters for solar neutrinos, θ_{Sun} and Δm^2_{Sun}, with θ_{12} and Δm^2_{21}, respectively; while for atmospheric neutrinos we identify θ_{atm} and Δm^2_{atm}, with θ_{23} and $\left|\Delta m^2_{32}\right| \simeq \left|\Delta m^2_{31}\right|$, respectively (experimentally it was observed that $\left|\Delta m^2_{32}\right| \simeq \left|\Delta m^2_{31}\right| \gg \left|\Delta m^2_{21}\right|$).

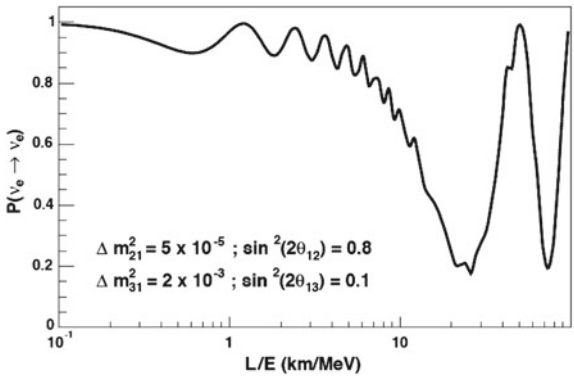

Fig. 9.10 ν_e survival probability as a function of L/E for fixed oscillation parameters as indicated in the figure. From http://www.hep.anl.gov/minos

The survival probability, for example, $\nu_e \to \nu_e$, in the case of three families is given by:

$$P\left(\nu_e \to \nu_e\right) = 1 - 4\left|U_{e1}\right|^2\left|U_{e2}\right|^2 \sin^2\left(\frac{\Delta m^2_{21}\, L}{4E_\nu}\right) +$$
$$-4\left|U_{e1}\right|^2\left|U_{e3}\right|^2 \sin^2\left(\frac{\Delta m^2_{31}\, L}{4E_\nu}\right) - 4\left|U_{e2}\right|^2\left|U_{e3}\right|^2 \sin^2\left(\frac{\Delta m^2_{32}\, L}{4E_\nu}\right).$$

The fact that $\left|\Delta m^2_{32}\right| \simeq \left|\Delta m^2_{31}\right| \gg \left|\Delta m^2_{21}\right|$ leads to an oscillation characterized by two different length scales. Indeed assuming that $\left|\Delta m^2_{32}\right| = \left|\Delta m^2_{31}\right|$, imposing unitarity and expressing the matrix elements in terms of the PMNS parametrization reported above, one obtains:

$$P\left(\nu_e \to \nu_e\right) \simeq 1 - \cos^4\left(\theta_{13}\right)\sin^2\left(2\theta_{12}\right)\sin^2\left(\frac{\Delta m^2_{21}\, L}{4E_\nu}\right) - \sin^2\left(2\theta_{13}\right)\sin^2\left(\frac{\Delta m^2_{32}\, L}{4E_\nu}\right). \tag{9.29}$$

In reactor experiments the energy of the neutrino (in fact $\overline{\nu}_e$) beams are of the order of a few MeV. Thus, as $\Delta m^2_{21} \sim 10^{-5} - 10^{-4}$ eV^2 and $\left|\Delta m^2_{32}\right| \sim 10^{-3}$ eV^2, experiments placed at distances of the order of the km are sensitive to θ_{13} while experiments placed at distances of the order of the hundreds of km are sensitive to θ_{12}.

This two-length behavior is illustrated in Fig. 9.10 where the probability of ν_e survival is shown for fixed oscillation parameters.

In the first case ($L \sim$ km) the above formula can be simplified to:

$$P\left(\overline{\nu}_e \to \overline{\nu}_e\right) \approx 1 - \sin^2\left(2\theta_{13}\right)\sin^2\left(\frac{\Delta m^2_{32}\, L}{4\, E_{\overline{\nu}}}\right) \tag{9.30}$$

while in the second case ($L \sim 100$ km) it can be simplified to:

$$P\left(\overline{\nu}_e \to \overline{\nu}_e\right) \approx 1 - \cos^4\left(\theta_{13}\right) \sin^2\left(2\theta_{12}\right) \sin^2\left(\frac{\Delta m^2_{21}\, L}{4\, E_{\overline{\nu}}}\right) . \tag{9.31}$$

9.1.7 *Short-Baseline Reactor Experiments, and the Determination of θ_{13}*

Close to a fission reactor, where the long wavelength oscillation did not develop yet, the electron antineutrino survival probability can be approximated as computed in Eq. 9.30.

The Daya Bay experiment in China is a system of six 20-ton liquid scintillator detectors (antineutrino detectors, AD) arranged in three experimental halls (EH), placed near six nuclear reactors (the geometry is shown in Fig. 9.11, left); as a consequence of the distances and of the geometry it is sensitive to short oscillations which may occur in a 3×3 mixing matrix scenario (see Sect. 9.1.6). In fact Daya Bay reported in March 2012 the first evidence of such short-scale oscillations (Fig. 9.11, right). Later, the RENO experiment in South Korea and Double Chooz in France confirmed such oscillations.

The best-fit values to all available data, including accelerator data (see Sect. 9.1.8), provide:

$$\sin^2\theta_{13} = 0.02203 \pm 0.00083 .$$

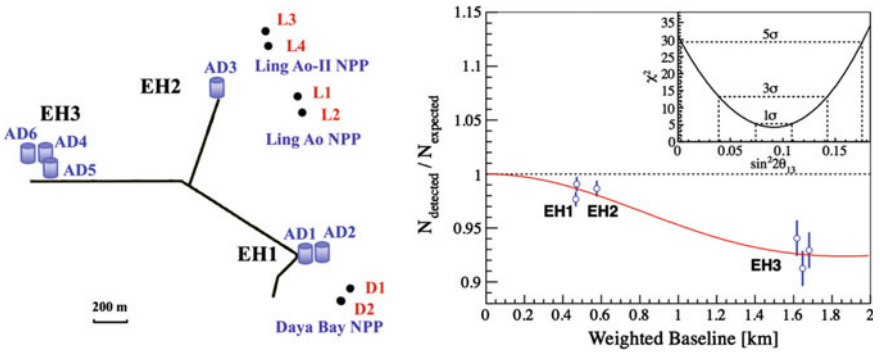

Fig. 9.11 Left: Layout of the Daya Bay experiment. The dots represent reactors, labeled as D1, D2, L1, L2, L3, and L4; the locations of the detectors are labeled EH1, EH2, and EH3. Right: The $\overline{\nu}_e$ disappearance as measured by the Daya Bay experiment. Ratio of the measured signal in each detector versus the signal expected assuming no oscillation. The oscillation survival probability at the best-fit $\sin^2 2\theta_{13}$ value is given by the smooth curve. The χ^2 versus $\sin^2 2\theta_{13}$ is shown in the inset. Figures from F.P. An et al., Phys. Rev. Lett. 108 (2012) 171803

Although small, a nonzero value of θ_{13} allows the phase $\delta \neq 0$ to produce *CP* violation in the neutrino sector.

9.1.8 *Accelerator Neutrino Beams*

The results from atmospheric neutrino experiments and reactor experiments can be tested in accelerator experiments, building intense and collimated ν_μ and $\overline{\nu}_\mu$ beams from the decay of secondary $\pi^\pm$ (and in a smaller percentage of $K^\pm$), and placing detectors both near (100–1000 m) and far (100–1000 km) from the primary target. The oscillation distance L is then fixed and the neutrino flux and the energy spectrum can be well predicted and precisely measured at the near detectors, constraining the elements of the neutrino mixing matrix.

The K2K (KEK to Kamioka) experiment, in Japan, was the first such experiment (actually its construction started at the end of the 1990s before the discovery of the neutrino oscillations in Super-Kamiokande). The neutrino beam, with a mean energy of 1.3 GeV, was produced at KEK in Tsukuba and the interactions were measured in a nearby detector at 300 m and in the Super-Kamiokande detector at 250 km (Fig. 9.12). 112 events were detected while 158 ± 9 where expected without considering oscillations; a neutrino oscillation pattern compatible with the atmospheric neutrino results was observed.

The T2K (Tokai to Kamioka) experiment followed K2K sending muon neutrinos to the Super-Kamiokande detector. It is a second-generation experiment located at 295 km from the accelerator. The neutrino beam, produced in the the J-PARC facility in Tokai, Eastern Japan, has a narrow range of energies around 600 MeV, selected in order to maximize the neutrino oscillation probability in their way to Super-Kamiokande. The intensity of the beam is two orders of magnitude larger

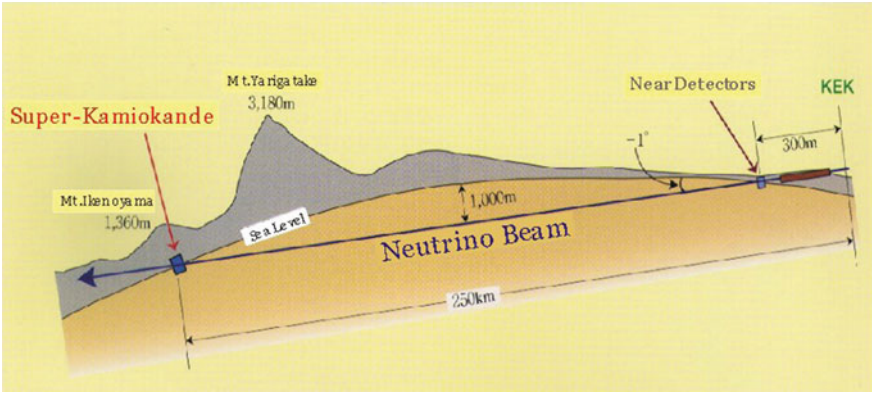

Fig. 9.12 Sketch of the neutrino path in the K2K long-baseline experiment. From http://neutrino.kek.jp

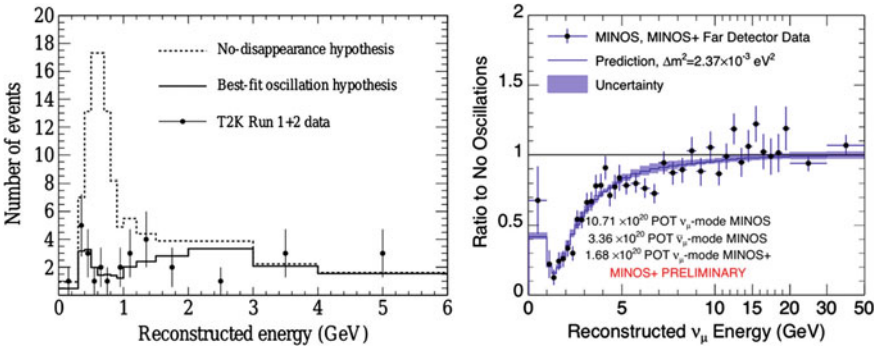

Fig. 9.13 Left: The first T2K study on the disappearance of muon neutrinos: muon-antineutrino events with well-reconstructed energy recorded before 2011. The energy distribution is compared to the calculations with and without oscillations. From Phys. Rev. D 85, 031103 (2012). Right: The ratio of the observed spectrum of muon neutrino interactions from MINOS to the predicted spectrum in the absence oscillations. The dark band represents the prediction assuming oscillations and its 1σ systematic uncertainty, using the best-fit oscillation parameters from MINOS. The observed data are well described by the oscillation model. From http://www-numi.fnal.gov/PublicInfo

than in K2K. The near detector (ND280), 280 m downstream the neutrino beam, is a segmented detector composed of neutrino targets inside a tracking system surrounded by a magnet. ND280 can measure the energy spectrum of the ν beam, its flux, flavor content, and interaction cross sections before the neutrino oscillation. We shall see later that, on top of precise measurements of the $\overline{\nu}_\mu$ disappearance (Fig. 9.13, left), T2K detected for the first time explicitly the appearance of $\overline{\nu}_e$ in a $\overline{\nu}_\mu$ beam.

In the USA, the MINOS experiment started taking data in 2005. The beam line at Fermilab is optimized to produce both ν_μ and $\overline{\nu}_\mu$ beams with a mean energy of 3 GeV. The far detector is placed at a distance of 735 km in the Soudan mine. A distortion of the energy spectrum at the far detector compatible with the previous oscillation measurements was observed for ν_μ beams (Fig. 9.13, right). More recently the NOνA experiment announced its first two years' results. NOνA is also a long-baseline (810 km) Fermilab experiment and is optimized to study ν_μ-disappearance and as ν_e-appearance in both neutrino and antineutrino channels.

These results can be once again interpreted in terms of oscillations in a two-flavor scenario (but now considering $\nu_\mu \rightarrow \nu_\tau$). They confirm and improve the result from the atmospheric neutrinos. The mixing is large and the mass difference is again much smaller than the normal fermion masses but much higher than the values measured in the case of the electron neutrino beam, i.e., in the "solar" neutrinos as discussed above. Accelerator and atmospheric experiments are complementary: in the former L is fixed and E known assuring a good resolution in the measurement of $\left|\Delta m^2_{23}\right|$ while in the latter the fluxes are high assuring a good resolution in the measurement of θ_{23}.

9.1.9 Explicit Appearance Experiment

The SNO experiment was somehow an appearance experiment: the comparison of charged-current events with neutral-current events provides an indication that μ plus τ neutrinos were present in the flux of solar neutrinos. Later, two experiments made an explicit detection of neutrinos of different flavor from the muon neutrinos in an accelerator beam.

The OPERA experiment located at Gran Sasso, Italy, receives a 17 GeV muon neutrino beam produced at CERN located 730 km away. OPERA uses a sophisticated 1200 tons detector composed by a sandwich of photographic emulsion films and lead plates in order to be able to detect tau-leptons: it is thus an appearance experiment aiming to detect tau-neutrinos resulting from the oscillation of the initial muon neutrino beam. OPERA, which concluded data-taking, reported five tau-neutrino candidates corresponding to significance of about 5σ; one of them is shown in Fig. 9.14.

T2K can make use of both muon neutrino and antineutrino beams from the same accelerator. Recent observation of the ν_e appearance from a high-purity ν_μ beam recorded 89 electron neutrino events while 67 events were expected in case of no *CP* violation; on the other hand, in a $\overline{\nu}_\mu$ beam 7 electron antineutrino events were detected while 9 events were expected in the case of no *CP* violation. The observed excess in the electron neutrino appearance rate and the observed smaller rate in the electron antineutrino appearance provides a 2σ indication of a possible difference in the oscillation parameters for neutrinos and antineutrinos which would imply a *CP* violation in the neutrino sector; this fact is reflected in the present result on the δ parameter (see Sect. 9.2).

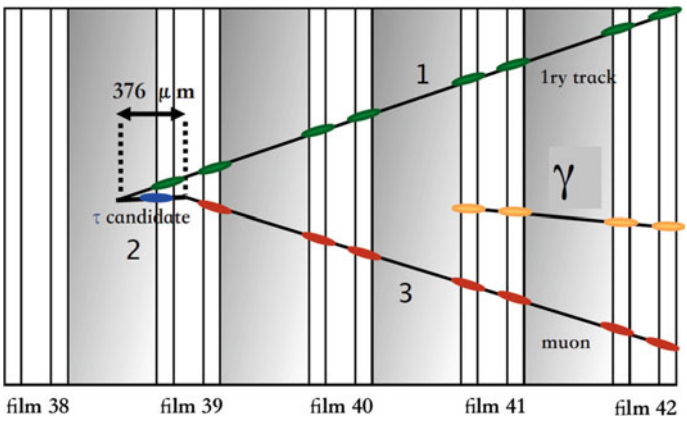

Fig. 9.14 One of the three tau neutrino candidate events observed by OPERA. From http://operaweb.lngs.infn.it

9.1.10 A Gift from Nature: Geo-Neutrinos

The interior of the Earth radiates heat at a rate of about 50 TW, which is about 0.1% of the incoming solar power. Part of this heat originates from the energy generated upon decays of radioactive isotopes, while another part is due to the cooling of the Earth.

The Earth's radioactive elements (in particular ^{238}U, ^{232}Th, ^{40}K) are β^- emitters and thus natural sources of $\overline{\nu}_e$, in this case designated as geo-neutrinos. The fluxes are small (as an example, around 21 events/year in KamLAND) but their measurement may provide important geological information on Earth's composition and structure that is not accessible by other means. The main backgrounds are due to nuclear reactors, since the contribution of atmospheric neutrinos is negligible and the Sun emits exclusively ν_e. KamLAND reported in 2013 a total observed signal of 116^{+28}_{-27} events and Borexino (a 280-ton liquid scintillator detector in Gran Sasso) reported recently the detection of a signal with a significance as high as 5.9 standard deviations. The current estimates are that, although with large errors, some 20 TW of power from the Earth comes from nuclear processes.

Thanks to neutrino detectors, a new highly interdisciplinary field, neutrino geophysics, has just been born.

9.2 Neutrino Oscillation Parameters

The simplified model in which neutrinos coming from two mass eigenstates oscillate between two flavors does not describe the full picture coming from the data. The large majority of the present experimental results are well described assuming three weak eigenstates (ν_e, ν_μ, ν_τ) and three mass eigenstates (ν_1, ν_2, ν_3).

Some researchers evidence a possible tension in the data, which for the first time was announced as the "LSND[5] anomaly." LSND claimed an oscillation with $|\Delta m| \sim 1$ eV, which would imply the existence of a neutrino with mass of at least one eV. The only way to accommodate this with the LEP results in the number of neutrino families is that this particle is a new kind of neutrino, which should be sterile–or at least not coupled to $W^\pm$ and Z.

The mixing matrix between three states is the Pontecorvo–Maki–Nakagawa–Sakata (PMNS) matrix (see Sect. 9.1.6). However, it should be noted that a complete treatment of neutrino propagation requires subtle questions of field theory and has close links to the foundation of quantum mechanics. Since different mass

[5]The Liquid Scintillator Neutrino Detector (LSND) was a 167-ton scintillation counter at Los Alamos National Laboratory that measured the flux of neutrinos produced by a near neutrino source, an accelerator beam dump.

components travel at different speeds, the mixing spreads the neutrino wavefunction in space, with EPR-like[6] implications.

The parameters of the PMNS matrix are: two mass differences (we can choose Δm^2_{21} and Δm^2_{31}); three angles (θ_{12}, θ_{23}, and θ_{13}); one single complex phase written in the form $e^{i\delta}$.

Data show that $|\Delta m^2_{31}| \gg |\Delta m^2_{21}|$. The sign of

$$\Delta M^2 \equiv m_3^2 - \frac{m_2^2 + m_1^2}{2} \,. \tag{9.32}$$

is not presently known: only the sign of Δm_{21} is determined to be positive from the experimental measurements (solar neutrinos). There are two possibilities (Fig. 9.15):

- $m_1 < m_2 < m_3$ (the so-called Normal Hierarchy or Ordering, NH or NO, ΔM^2 positive);
- $m_3 < m_1 < m_2$ (the so-called Inverted Hierarchy or Ordering, IH or IO, ΔM^2 negative).

Results are usually presented in terms of the variable $\Delta m^2_{3\ell}$, with $\ell = 1$ for NH and $\ell = 2$ for IH. Hence, $\Delta m^2_{3\ell} = \Delta m^2_{31} > 0$ for NH and $\Delta m^2_{3\ell} = \Delta m^2_{32} < 0$ for IH; i.e., it corresponds to the mass splitting with the largest absolute value. Best-fit values of the mass differences and of the mixing angles imposing unitarity of the mixing matrix and, in case the difference between the NH and the IH hypothesis is smaller than half the error, averaging the two values and increasing the error itself by the absolute half difference of the two values, are:

$$\Delta m^2_{21} = \left(74.0^{+2.1}_{-2.0}\right) \times 10^{-6}\text{eV}^2 = (8.60 \pm 0.12\,\text{meV})^2 \tag{9.33}$$

$$|\Delta m^2_{3\ell}| = (24.99 \pm 0.50) \times 10^{-4}\text{eV}^2 = (50.0 \pm 0.5\,\text{meV})^2 \tag{9.34}$$

$$\sin^2\theta_{12} = 0.307 \pm 0.013 \tag{9.35}$$

$$\sin^2\theta_{23} = 0.568 \pm 0.028 \tag{9.36}$$

$$\sin^2\theta_{13} = 0.02203 \pm 0.00083\,. \tag{9.37}$$

The complex phase is

$$\delta = \left(228^{+51}_{-33}\right)^\circ \ (NH)\ ;\ \delta = \left(281^{+30}_{-33}\right)^\circ \ (IH)\,. \tag{9.38}$$

Data provide a marginal indication of violation of *CP* in the neutrino sector, but there is not yet sensitivity to confirm firmly this hypothesis—values of $\sin\delta$ are consistent with zero within 3σ. Anyhow, the current best-fit value for δ, even with these very large errors, is close to $(3/2)\pi$ which would imply a maximal *CP* violation. This

[6]The Einstein–Podolski–Rosen (EPR) paradox originally involved two particles, A and B, which interact briefly and then move off in opposite directions. The two particles are then entangled, and any measurement on A (projection of A on an eigenstate) would have *immediately* implications on the state of B; this would violate locality. In the case of neutrinos, the neutrino wavefunction itself spreads during the travel, with possible nonlocal effects.

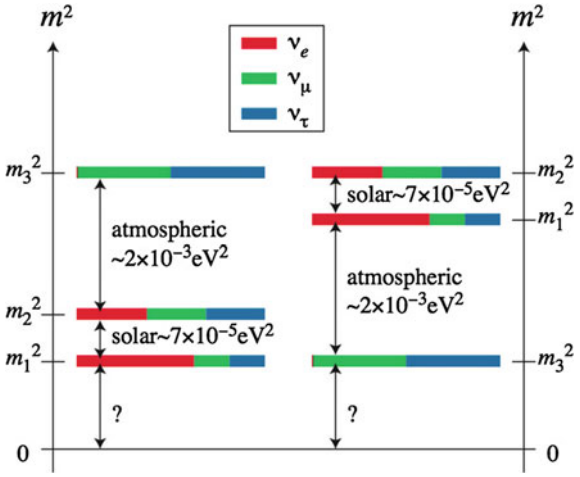

Fig. 9.15 Diagram of the relationship between the mass eigenstates (labeled 1, 2, and 3) for neutrinos and the flavor eigenstates (ν_e, ν_μ, ν_τ). Neutrinos from the Sun have been used to determine the relation between m_2 and m_1; m_3 may be greater or smaller than m_1 and m_2. The fractional contribution of each flavor to the mass eigenstates is indicted by the colored bars. Updated from S.F. King, arXiv:0712.1750

could help, through the leptogenesis mechanisms, to explain the matter-antimatter asymmetry in the Universe.

The PMNS matrix is highly nondiagonal, which is very different from what it is observed in the quark sector (see Sect. 6.3.7). The best estimates of 3σ confidence intervals for its elements are (NuFIT 2017):

$$\begin{pmatrix} \nu_e \\ \nu_\mu \\ \nu_\tau \end{pmatrix} = \begin{pmatrix} 0.799 \to 0.844 & 0.516 \to 0.582 & 0.140 \to 0.156 \\ 0.234 \to 0.502 & 0.452 \to 0.688 & 0.626 \to 0.784 \\ 0.273 \to 0.527 & 0.476 \to 0.705 & 0.604 \to 0.765 \end{pmatrix} \begin{pmatrix} \nu_1 \\ \nu_2 \\ \nu_3 \end{pmatrix} . \quad (9.39)$$

Future facilities are planned to improve our knowledge of the mixing matrix and possibly discover new physics; in particular, high-precision and high-luminosity long-baseline neutrino oscillation experiments have been proposed in the USA, in Japan, and in Europe.

9.3 Neutrino Masses

The discovery of neutrino oscillations showed, as discussed above, that the neutrino flavor eigenstates are not mass eigenstates and at least two of the mass eigenstates are different from zero.

Thanks to a huge experimental effort, we know quite well the neutrino mass differences. As of today we do not know, however, the absolute values of the neutrino masses. The value of $\Delta m^2_{3\ell}$ (Eq. 9.34) suggests masses of the order of 1–100 meV; a lower limit

$$\sum m_{\nu_i} > 60 \text{ meV} \quad (9.40)$$

can be extracted at 95% C.L. from the data discussed in the previous Section.

However, the possibility that the mass of the lightest neutrino is much larger than this and that all three known neutrino masses are quasi-degenerate is not excluded.

Neutrino masses can only be directly determined via nonoscillation neutrino experiments. The most model-independent observable for the determination of the mass of the electron neutrino is the shape of the endpoint of the beta decay spectrum. Other probes of the absolute value of the neutrino masses include double beta decays, if neutrinos are of Majorana type, discussed below, and maps of the large-scale structure of the Universe, which is sensitive to the masses of neutrinos—although this sensitivity depends on cosmological models.

9.3.1 The Constraints from Cosmological and Astrophysical Data

The neutrino mass is constrained by cosmological data. Indeed neutrinos contribute to the energy density of the Universe playing the role of "hot dark matter." The combined analyses of the CMB data and of the surveys of the large-scale structures in the Universe (see Chap. 8) set a limit on the sum of the mass of the three neutrino species to

$$\sum m_{\nu_i} < 0.23 \text{ eV} \tag{9.41}$$

at 95% C.L. A more conservative limit

$$\sum m_{\nu_i} < 0.68 \text{ eV} \tag{9.42}$$

can be extracted as follows, based on the density and sizes of structures in the Universe. Initial fluctuations seeded the present structures in the Universe, growing during its evolution. Neutrinos, due to their tiny masses, can escape from most structures being their speed larger than the gravitational escape velocity. As a net result, neutrinos can erase the structures at scales smaller than a certain value D_F called the free streaming distance. The smaller the sum of the neutrino masses, the larger is D_F. The relevant observable is the mass spectrum, i.e., the probability of finding a structure of a given mass as a function of the mass itself. Cosmological simulations predict the shape of the mass spectrum in terms of a small number of parameters; the limit in Eq. 9.42 is the limit beyond which the predicted distribution of structures is inconsistent with the observed one.

Data from astrophysical neutrino propagation over large distances are less constraining. So far the only reported upper limit on the neutrino velocity was obtained comparing the energy and the arrival time of a few tens of neutrinos by three different experiments from the explosion of the supernova 1987 A in the Large Magellanic Cloud at around 50 kpc from Earth. From these results a limit of about 6 eV was

obtained on the masses of the neutrinos reaching the Earth. The present long-baseline accelerator experiments are not sensitive enough to set competitive limits.

9.3.2 Direct Measurements of the Electron Neutrino Mass: Beta Decays

The study of the energy spectrum of the electrons produced in nuclear β decays is, one century after the first measurement, still the target of intense experimental efforts. In particular, the detailed measurement of the endpoint of this spectrum may allow the determination of the electron neutrino mass by direct energy conservation.

In fact it can be shown that whenever the parity of the initial and the final nuclei is the same, the spectrum of the outgoing electron is given by:

$$\frac{dN}{dE} = \frac{G_F^2 \cos^2\theta_c I^2}{2\pi^3} F(Z,R,E)\,|\mathbf{p}|\,E\,(E_0 - E)\sqrt{(E_0 - E)^2 - m_{\nu_e}^2} \tag{9.43}$$

where:

1. $\cos\theta_c$ is the cosine of the Cabibbo angle.
2. I is an isospin factor that depends on the isospin of the initial and the final nucleus.
3. $F(Z,R,E)$ is the "Fermi function" accounting for the electrostatic interaction between the nuclei and the outgoing electron which depends on the nuclear charge Z, on the nuclear radius R and the electron energy.
4. $E_0 \simeq Q = M(Z,A) - M(Z+1,A) - m_e$ is the total energy available for the electron and the antineutrino.

The endpoint of this spectrum can then be graphically determined plotting the quantity $K(E)$ (Kurie plot, Fig. 9.16, left), where

$$K(E) = \frac{dN/dE}{F(Z,R,E)\,|\mathbf{p}|\,E}\,. \tag{9.44}$$

In the case of $m_{\nu_e} = 0$

$$K(E) \propto (E_0 - E) \tag{9.45}$$

and the plot is just a straight line. However, if $m_{\nu_e} \neq 0$, this line bends slightly near the endpoint (Fig. 9.16) and $K(E)$ becomes null at:

$$E = E_0 - m_{\nu_e}\,. \tag{9.46}$$

Assuming a mixing scenario with three nondegenerate mass eigenvalues the spectrum at the endpoint would be the superposition of the Kurie plots corresponding to each of the mass eigenvalues (Fig. 9.16, right); indeed the measured mass will be a superposition m_β such that

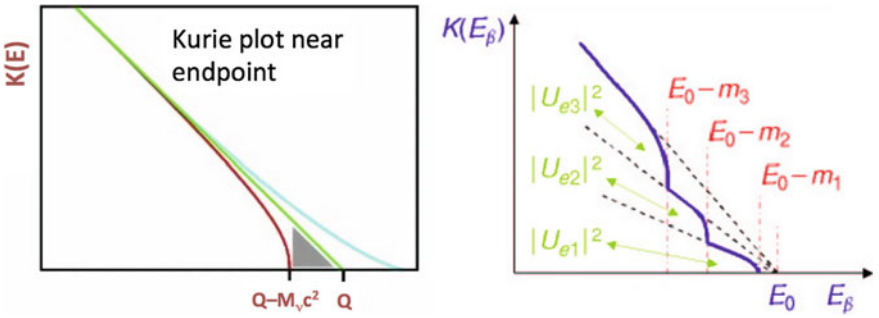

Fig. 9.16 Left: Kurie plot. The green line represents the ideal case for $m_{\nu_e} = 0$, the red line the ideal case for $m_{\nu_e} \neq 0$, and the blue line the real case where a finite detector resolution introduces a smearing at the endpoint. Right: Detail of the endpoint in case of a mixing scenario with three nondegenerated mass eigenvalues. Andrea Giuliani, "Review of Neutrino Mass Measurements," Quark–Lepton conference Prague, 2005

$$m_\beta^2 = \sum |U_{ei}^2| m_i^2 \,. \tag{9.47}$$

Two nuclides are of major importance to current β decay experiments: tritium and ^{187}Re. The physics is the same in both cases, but the experimental technique differs. Tritium has a relatively high Q-value of 18.6 keV which makes the detection of the electron easier in the process $^3\mathrm{H} \rightarrow {}^3\mathrm{He} + e^- + \bar{\nu}_e$; the detection of electrons from ^{187}Re (with a 2.5 keV Q-value) needs a micro-calorimeter embedded in the radioactive material.

The best present results were obtained by experiments (Troitsk in Russia and Mainz in Germany) using tritium as a source. These experiments measure the electron energy using complex magnetic and electrostatic spectrometers. The current limit at 95% C.L. (PDG2017) is:

$$m_{\nu_e} < 2.0\,\mathrm{eV}. \tag{9.48}$$

Following this line an ambitious project (KATRIN in Karlsruhe, Germany) having a 200-ton spectrometer is presently in preparation. KATRIN aims either to improve this limit by an order of magnitude or to measure the mass, with a sensitivity of 0.2 eV. An alternative proposal (Project 8 in Yale, US) is to use the measurement of the cyclotron frequency of individual electrons to reach similar sensitivities.

9.3.3 *Direct Measurements of the Muon- and Tau-Neutrino Masses*

The muon and the tau neutrino masses were studied, respectively, in the decays of charged pions ($\pi^+ \rightarrow \mu^+ \nu_\mu$ and $\pi^- \rightarrow \mu^- \overline{\nu}_\mu$), and in the three- and five-prongs decays of the tau lepton. Limits

$$m_{\nu_\mu} < 0.19\,\text{MeV} \tag{9.49}$$

and

$$m_{\nu_\tau} < 18.2\,\text{MeV} \tag{9.50}$$

were obtained at 95% confidence level. However, they are not competitive either with the cosmological limits or with the combination of the direct m_{ν_e} limit with the limits on the square mass differences (Δm^2_{ij}) from the study of neutrino oscillations (see the previous sections).

9.3.4 Incorporating Neutrino Masses in the Theory

The first formulation of the standard model had to be extended to accommodate neutrino masses.

The most straightforward solution is to introduce in the SM Lagrangian mass terms for the neutrinos similar to the existing for the other fermions:

$$-\frac{g_\nu}{\sqrt{2}} v\,(\overline{\nu}_L \nu_R + \overline{\nu}_R \nu_L) \tag{9.51}$$

where g_ν is the Yukawa coupling, $v = 246$ GeV is the Higgs vacuum expectation value, and ν_L and ν_R are, respectively, the left- and right-handed chiral[7] Dirac spinors. This mass term is built with the normal Dirac spinors and so these neutrinos are designated as Dirac neutrinos. The right-handed neutrino that was not necessary in the first formulation of the SM should then exist. In fact, in the case of massless neutrinos chirality is conserved and as the right-handed neutrino is a SU(2) singlet and has no weak interactions, as well as no strong and electromagnetic interactions: excluding gravitational effects, it is invisible.

However neutrinos and antineutrinos have, apart from the lepton number which is not generated by a fundamental interaction symmetry, the same quantum numbers and thus they can be the same particle. This would not be possible in the case of the electrons/positrons, for example, as they have electric charge.

The neutrino and the antineutrino can, in this hypothesis first introduced by Ettore Majorana in 1937, be described only by two-component chiral spinors (instead of the four-component spinors in the case of the Dirac fermions).

In this frame a left-handed neutrino is identical (but for a phase) to a right-handed antineutrino which may be described by the *CP* conjugate of the left-handed neutrino (ν_L^C). A mass term involving left-handed neutrinos and right-handed antineutrinos can then be written:

$$-\frac{1}{2} m \left(\overline{\nu}_L \nu_L^C + \overline{\nu_L^C} \nu_L\right) . \tag{9.52}$$

[7]Hereafter in this section the designations "left"- and "right-handed" refer to chirality and not to helicity. Note that for massive neutrinos chirality and helicity are not equivalent (see Chap. 6).

However, $\overline{\nu_L^C}\nu_L$ has weak hypercharge $Y = -2$ and thus cannot make a gauge invariant coupling with the standard model Higgs doublet which has $Y = +1$. To accommodate such a term an extension of the Higgs sector would be therefore needed.

An alternative would be to introduce again right-handed neutrinos (designated now as Majorana neutrinos). In this scenario, a left-handed antineutrino is identical (but for a phase) to a right-handed neutrino and may be described by the *CP* conjugate of the right-handed neutrino (ν_R^C). Mass terms involving right-handed neutrinos and left-handed antineutrinos,

$$-\frac{1}{2}M\left(\overline{\nu_R^C}\nu_R + \overline{\nu}_R\nu_R^C\right) \tag{9.53}$$

are then SU(2) singlets and they can be introduced directly in the Lagrangian without breaking the gauge invariance. No Higgs mechanism is therefore needed in this scenario in the neutrino sector. These Majorana neutrinos would not couple to the weak bosons.

Both Dirac and Majorana mass terms may be present. In the so-called see-saw mechanism, a Dirac term with mass m_D and a Majorana term with mass M as defined above are introduced. The physical states for which the mass matrix is diagonal are now a light neutrino with mass

$$m_\nu \sim \frac{m_D^2}{M} \tag{9.54}$$

and a heavy neutrino with mass

$$m_N \sim M\,. \tag{9.55}$$

The interested reader can find the explanation in the additional material.

The light neutrino, in the limit of $M \gg m_D$, has the same couplings as the standard model neutrinos, while the heavy neutrino is right-handed and thus sterile and may have a role in the Dark Matter problem.

The extremely small values that experiments indicate for the neutrino masses are in this way generated thanks to the existence of a huge Majorana mass, while the scale of the Dirac mass would be the same as for the other fermions. The introduction of Majorana neutrinos may also help, via leptogenesis and *CP* violation, to explain the matter-antimatter asymmetry present in the Universe. These heavy neutrinos may be experimentally detected in present (LHC, NA62, T2K, …) or future experiments like SHiP or in future lepton or proton colliders.

9.3.5 Majorana Neutrinos and the Neutrinoless Double Beta Decay

If Majorana neutrinos do exist (i.e., if neutrinos and antineutrinos are the same particle), neutrinoless double β decays ($0\nu\beta\beta$, also called $\beta\beta0\nu$) can occur, in particular

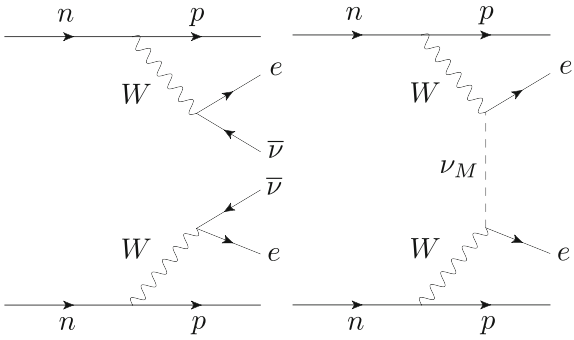

Fig. 9.17 Double β decay diagrams: on the left the case of Dirac neutrinos characterized by a final state with two $\overline{\nu}_e$; on the right the neutrinoless β decay allowed in the case of Majorana neutrinos

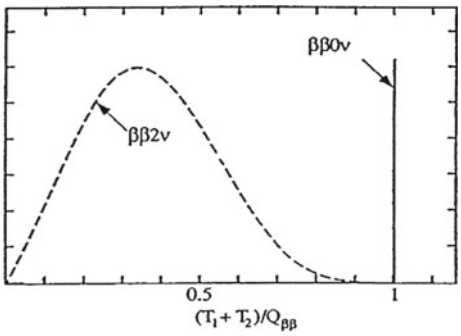

Fig. 9.18 Energy spectrum of the sum of the two electrons in the case of the double β decay of a nucleus with (broad distribution) or without (line) $\overline{\nu}_e$ emission

for nuclei for which the normal β decays are forbidden by energy conservation. The lines corresponding to the emission of the $\overline{\nu}_e$ can be connected becoming an internal line (Fig. 9.17).

Considering that the nuclei before and after the decay are basically at rest, the sum of the energies of the two electrons in $0\nu\beta\beta$ decays is just the difference of the masses of the two nuclei ($Q = M(Z, A) - M(Z + 2, A) - 2m_e$). Thus in these decays the energy spectrum of the emitted electrons should be a well-defined line while in the normal double β decay, with the emission of two $\overline{\nu}_e$, this spectrum accommodates a large phase space and the electron energy distribution is broad (Fig. 9.18).

The decay rate is proportional to the square of the sum of the several mass eigenstate amplitudes corresponding to the exchange of the electron (anti)neutrino (coherent sum of virtual channels). Then it is useful to define an effective Majorana mass as:

$$m_{\beta\beta} = \left| \sum |U_{ek}|^2 e^{i\alpha_k} m_k \right| \tag{9.56}$$

where α_i are the Majorana phases (one of them can be seen as a global phase and be absorbed by the neutrino wavefunctions but the two remaining ones cannot be absorbed, as it was the case for Dirac neutrinos).

Being a function both of the neutrino masses and of the mixing parameters, this effective mass depends on the neutrino mass hierarchy. In the case of the normal

hierarchy total cancellation may occur for given range of masses of the lightest neutrino and $m_{\beta\beta}$ may be null.

The experimental measurement is extremely difficult due to the low decay rates and the backgrounds. An ideal experiment should then have a large source mass and an excellent energy resolution; a clean environment and techniques to suppress the background (such as particle identification, spatial resolution, and timing information) would help in general.

Several experimental strategies have been implemented in the last years, and eleven isotopes for which single beta decay is energetically forbidden have been experimentally observed undergoing double beta decay, for which half-lives (typically of the order of 10^{21} years) have been measured. Among the most interesting double beta decay emitters are:

- ^{136}Xe, with a high Q-value of about 2.5 MeV where background is small, which can can be dissolved in liquid scintillators or used as gas for a homogeneous detector providing both scintillation and ionization signals (this technique is exploited by the Enriched Xenon Observatory EXO, installed near Carlsbad, New Mexico, and by KamLAND-Zen in Kamioka).
- ^{76}Ge, which can be embedded in solid-state detectors (GERDA at Gran Sasso and Majorana in the Sanford Underground Research Facility SURF, South Dakota).
- ^{130}Te, which has a large natural abundance and can be used to build a bolometric detector (experiment CUORE at LNGS). Bolometers measure the energy released by a particle using the change in the electric resistance induced by the heating of a crystal at very low (mK) temperatures. ^{130}Te can be also dissolved in liquid scintillators (experiment SNO+).

No confirmed signal was so far established (limits for $m_{\beta\beta}$ of a few hundred meV were obtained from the limits on the neutrinoless half-lives). In the next years, the new generation of experiments may reach the inverted hierarchy mass region.

9.3.6 Present Mass Limits and Prospects

The present results from the oscillation and cosmological data set already strong constrains in the plane ($\sum m_{\nu_i}$,$m_{\beta\beta}$) as shown in Fig. 9.19.

The present limits for $0\nu\beta\beta$ decays experiments are too high to restrict the allowed phase space region but sensitivities as low as 0.02–0.05 eV may be reached in a few years by the next-generation $0\nu\beta\beta$ experiments. In what concerns m_{ν_i} direct measurements, KATRIN will explore in the next years the m_β region up to sensitivities of $\sim$0.2 eV, which is unfortunately too high to exclude the IH scenario. However, long-baseline experiments may, in the next years, be able to disentangle the two scenarios.

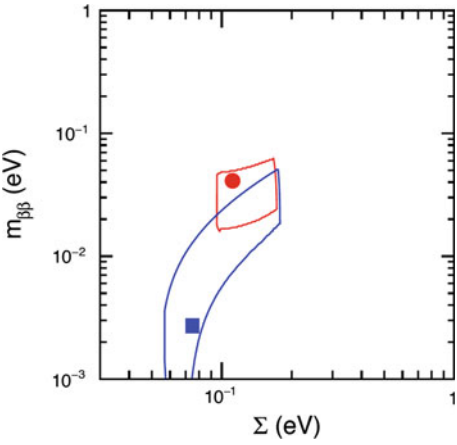

Fig. 9.19 2σ confidence regions in the plane $(\sum m_{\nu_i}, m_{\beta\beta})$ in the NH (blue, with a square inside) and IH (red, with a circle inside) scenarios. Figure adapted from F. Capozzi et al., "Global constraints on absolute neutrino masses and their ordering," Phys. Rev. D95 (2017) 096014

Further Reading

[F9.1] C. Giunti and C.W. Kim, "Fundamentals of Neutrino Physics and Astrophysics", Oxford 2007.

Exercises

1. *Neutrino interaction cross section.* Explain the peak in the cross section in Fig. 9.1.
2. *Neutrinos from the Sun.* Neutrinos from the Sun come mostly from reactions which can be simplified into

$$4p \rightarrow {}^4\mathrm{He} + 2e^+ + 2\nu_e\,.$$

   The energy gain per reaction corresponds to the binding energy of He, ~28.3 MeV. The power of the Sun at Earth (nominal solar constant) is P = 1361 W/m^2. How many solar neutrinos arrive at Earth per square meter per second?
3. *Radiation exposure due to solar neutrinos.* If the the neutrino–nucleon cross section in the energy range for solar neutrinos is approximately 10^{-45} cm^2/nucleon, (a) compute the rate of interactions of solar neutrinos in the human body, assuming that the human body has the density of water. (b) If neutrinos interact with nucleons N in the human body by the process $\nu N \rightarrow eN'$, and radiation damage is caused by electrons, estimate the annual dose for a human with mass of 80 kg under the assumption that on average 50% of the neutrino energy is transferred to the electron, and that the average energy of neutrinos is 100 keV.
4. *Neutrino oscillation probability.* Given a pure muon neutrino beam, with fixed energy E, derive the probability of observing another neutrino flavor at a distance L assuming two weak eigenstates related to two mass eigenstates by a simple rotation matrix.
5. *Tau neutrinos appearance.* OPERA is looking for the appearance of tau neutrinos in the CNGS (CERN neutrinos to Gran Sasso) muon neutrino beam. The average

neutrino energy is 17 GeV and the baseline is about 730 km. Neglecting mass effects, calculate the oscillation probability

$$P(\nu_\mu \to \nu_\tau)$$

and comment.

6. *Neutrino mass differences.* A neutrino experiment detects, at 200 m from the nuclear reactor that the flux of a 3 MeV antineutrino beam is $(90 \pm 10)\%$ of what was expected in case of no oscillation. Assuming a maximal mixing determine the value of Δm^2_ν.
7. *Neutrino rotation angles.* Suppose there are three neutrino types (electron, muon, tau) and three mass values, related by the 3×3 PMNS matrix, usually factorized by three rotation matrices. Knowing that the three mass values are such that:
   - Δm^2 (solar) $= m_2^2 - m_1^2 \sim 10^{-5}\text{eV}^2$
   - Δm^2 (atmospheric) $= \left|m_3^2 - m_2^2\right| \sim 10^{-3}\text{eV}^2$

   discuss the optimization of reactor and accelerator experiments to measure each of the three rotation angles and to confirm such mass differences. Compare, for example, the pairs of experiments (KamLAND, DayaBay), (T2K, OPERA).
8. *Neutrino from Supernova 1987A.* In 1987, a Supernova explosion was observed in the Magellanic Cloud, and neutrinos were measured in three different detectors. The neutrinos, with energies between 10 and 50 MeV, arrived with a time span of 10s, after a travel distance of 5×10^{12} s, and 3 h before photons at any wavelength.
   (a) Can this information be used to determine a neutrino mass? Discuss the quantitative mass limits that could be derived from the SN1987A.
   (b) This was the only SN observed in neutrinos, up to now, but the same reasoning can be used in pulsed accelerator beams. Derive the needed time and position precision to measure $\sim$1 eV masses, given a beam energy $E \sim 1$ GeV and distance L.
9. *Double β decay.* Double β decay is a rare process, possible only for a small fraction of the nuclear isotopes. The neutrinoless double β decay is only possible if lepton number is not conserved, and is one of the most promising channels to discover lepton number violation. Discuss the optimization (total mass, chosen isotope, backgrounds, energy resolution, …) of the experiments looking for $0\nu\beta\beta$. List other possible experimental signals of lepton number violation you can think of.